

Article

Vulnerability Analysis of Geographical Railway Network under Geological Hazard in China

Lingzhi Yin ¹, Jun Zhu ^{2,*}, Wenshu Li ¹ and Jinhong Wang ³

¹ School of Information Science and Technology, Zhejiang Sci-Tech University, Hangzhou 310018, China; linzyhn@zstu.edu.cn (L.Y.); charlie@zstu.edu.cn (W.L.)

² Faculty of Geosciences and Environmental Engineering, Southwest Jiaotong University, Chengdu 611756, China

³ Zhejiang Academy of Surveying and Mapping, Hangzhou 311100, China; wangjinhong32@yeah.net

* Correspondence: zhujun@swjtu.edu.cn

Abstract: As the passenger railway network is expanding and improving, the internal connections and interdependence in the network are rising. Once a sudden geological hazard occurs and damages the network structure, the train service is prone to large-scale halt or delay. A geographical railway network is modeled to analyze the spatial distribution characteristics of the railway network as well as its vulnerability under typical geological hazards, such as earthquakes, collapses, landslides and debris flows. First, this paper modeled the geographical railway network in China based on the complex network method and analyzed the spatial distribution characteristics of the railway network. Then, the data of geological hazards along the railway that occurred over the years were crawled through the Internet to construct the hazard database to analyze the time–space distribution characteristics. Finally, based on the data of geological hazards along the railway and results of the susceptibility to geological hazards, the vulnerability of the geographical railway network was evaluated. Among these geological hazards, the greatest impact on railway safety operation came from earthquakes (48%), followed by landslides (28%), debris flows (17%) and collapses (7%). About 30% of the lines of the geographical railway network were exposed in the susceptibility areas. The most vulnerable railway lines included Sichuan–Guizhou Railway, Chengdu–Kunming Railway and Chengdu–Guiyang high-speed Railway in Southwest China, Lanzhou–Urumqi Railway and Southern Xinjiang Railway in Northwest China, and Beijing–Harbin Railway and Harbin–Manzhouli Railway in Northeast China. Therefore, professional railway rescue materials should be arranged at key stations in the above sections, with a view to improving the capability to respond to sudden geological hazards.



Citation: Yin, L.; Zhu, J.; Li, W.; Wang, J. Vulnerability Analysis of Geographical Railway Network under Geological Hazard in China. *ISPRS Int. J. Geo-Inf.* **2022**, *11*, 342. <https://doi.org/10.3390/ijgi11060342>

Academic Editors: Wolfgang Kainz and Godwin Yeboah

Received: 11 April 2022

Accepted: 8 June 2022

Published: 10 June 2022

Publisher's Note: MDPI stays neutral with regard to jurisdictional claims in published maps and institutional affiliations.



Copyright: © 2022 by the authors. Licensee MDPI, Basel, Switzerland. This article is an open access article distributed under the terms and conditions of the Creative Commons Attribution (CC BY) license (<https://creativecommons.org/licenses/by/4.0/>).

1. Introduction

Railway transportation has played a vital role in the national economy, underpinning the deep economic ties and transportation for interaction. Compared to other means of transportation, it has the advantages of huge carrying capacity, low operation cost, long distance and all weather [1–3]. With rapid economic development and a continuous rise in population, there is an increasing demand for travel and a higher requirement for the carrying capacity of the passenger railway [4–6]. Since 2005, China has vigorously developed high-speed trains to relieve transportation pressure. As of 2021, the national operating railway mileage reached 146,000 km, of which high-speed railway accounted for 38,000 km [7]. Looking forward to 2030, China's passenger railway network system will basically achieve internal and external interconnection, smooth transportation through multi-roads between regions, the connection of different provincial capitals through high-speed rail, rapid access to cities and counties and basic railway coverage of counties [8,9]. With the improvement in the passenger railway network, the internal connections of the

network have gradually increased, and the degree of interdependence has also increased. Once a sudden geological hazard occurs and damages the network structure, the railway operation will be affected, causing train delays and cancellations. It will even paralyze the railway network structure and seriously affect the national economic production and people's daily travel [10–12].

China has a vast territory and complex terrain. Railway lines often have to pass through extreme terrain and have to face various types of sudden geological hazards, such as earthquakes, debris flows, collapses and landslides [1,13,14]. The occurrence of geological hazards will not only affect the running organization of the railway, but also bring great harm to the life and safety of passengers [15–17]. For example, the Wenchuan earthquake in May 2008 caused several landslides in Baoji–Chengdu Railway, Chengdu–Kunming Railway and related branch lines. Stations and railway facilities along the lines were damaged to varying degrees, making it difficult for rescue workers and equipment to reach the worst-hit areas, and seriously undermining the speed of hazard relief [18]. In August 2019, affected by continuous rainfall in parts of Sichuan province, a landslide occurred between Lianghong Station and Aidai Station on the Chengdu–Kunming Railway, causing the halt of the line and 17 rescuers lost their lives at the scene [19]. In March 2020, debris flows and landslides triggered by continuous rainfall in Chenzhou, Hunan province, caused a T179 Jinan–Guangzhou passenger train to derail and roll over, resulting in 1 fatality, 4 severe casualties and over 120 injuries [20]. Therefore, it is pressing to comprehensively and effectively evaluate the vulnerability of passenger railway network systems under geological hazards, identify the lines that are easily affected by geological hazards and carry out risk-prevention work in advance.

Based on the theory of complex network and linear reference, a geographical railway network was built in this paper. Taking the impact on the overall railway network efficiency as the vulnerability index, the vulnerability of the railway network under various geological hazards was analyzed. The research provides a basis for ensuring the normal operation and enhancing the hazard defense and mitigation ability of China's railway system.

2. Literature Review

Margat first proposed the term “groundwater vulnerability”, which was interpreted as the self-protection of groundwater against pollutants [21]. Since then, the concept has been widely used in public health, land use, economics, sustainability science and other fields. The connotation of vulnerability has gradually evolved from the inherent vulnerability of natural systems alone to a broader integrated concept of natural and social systems. In the meantime, the research thereon has extended from the initial concern about the vulnerability of the natural environment alone to discussions on the vulnerability of humanity and the human–environment coupled system. Due to the differences among the application fields in research objects and disciplinary perspectives, different disciplines adopt very different definitions, perspectives, understanding and connotations of “vulnerability”. Timmerman regarded vulnerability as the degree to which a system would respond adversely to a hazard event [22]. Brooks took vulnerability as a complex relationship of the interaction of components, such as exposure, susceptibility and adaptability, at different spatial scales [23]. Birkmann et al. proposed a framework for vulnerability assessment adapted to hazard risk management and climate change. The framework has promoted discussions on defining vulnerability, hazard risk, risk management and adaptation and the connections between these concepts [24].

Vulnerability of the transportation system is closely related to our everyday life. However, there is not yet a definite and unified concept of transportation vulnerability. The research on the vulnerability and reliability of transportation originated from the 1995 Hanshin Earthquake [25]. Berdica was the first to propose a definition of the vulnerability of the transportation network; it was considered to be a sensitive factor susceptible to events and would cause the service standard of the road transport network to be greatly reduced [26]. Hu et al. defined traffic vulnerability as the degree of sensitivity of the traffic state to a

series of problems caused by external disturbances and influences [27]. Erath et al. studied the vulnerability of the Swiss transportation system and thereby, expressed vulnerability as the product of the probability of a segment failure in a hazardous situation, multiplied by the sum of the direct and indirect consequences of the interruption [28]. Mattsson et al. provided a broader socio-technical perspective; namely, it is the ability of a transportation system to maintain or quickly restore its function after a disruption or hazard [29].

As the theory of complex networks infiltrates into various disciplines, many scholars have studied the network characteristics and vulnerabilities of the transportation network in urban road transportation, rail transit, railway networks and public transportation networks. In a complex network, vulnerability refers to the drop in network efficacy when there is an emergency. Albert et al. were the first to study the anti-hazard capability of networks in cases of random failure (removal of some randomly selected nodes) and deliberate attack (removal of the nodes with maximum degree or maximum betweenness) [30]. Based on percolation theory, Cohen et al. studied the critical proportion of node removal that would lead to the complete collapse of the network under random attack and presented the analytical expression [31]. Berche et al. took buses, metro, trams, ferries, etc., as a large transportation system and analyzed vulnerabilities in public transport systems in 14 cities in cases of random failure and deliberate attack [32]. Wu et al. mainly discussed the topological characteristics of the public transport system in Beijing and elaborated the vulnerability of the public transport system in the face of accidents and attacks [33]. Kermanshah et al. provided a geographical and multi-criteria vulnerability assessment method to quantify the impacts of extreme earthquakes on road networks [34]. Candelieri et al. provided network analysis functionalities for vulnerability assessment in public transportation networks with respect to disruptive events and/or targeted attacks to stations [35].

As the main artery of the national economy and one of the main modes of transportation in the comprehensive traffic and transportation system, the railway transportation system has also become a focus in the field of vulnerability research. Ouyang et al. compared the complex system-based railway system model and the actual train-flow-based railway system model and analyzed their respective vulnerability [1]. Pant et al. adopted a networks approach to modelling interdependent critical infrastructures and building a vulnerability assessment framework [36]. Meesit et al. assessed the vulnerability of the railway network in the East Midlands of the United Kingdom through randomized microsimulation [37]. Szymula et al. proposed a model of railway network vulnerability that assessed the system vulnerability by locating the key link combination causing the most adverse consequence for the passengers and trains [12]. However, these studies only adopt the random attacks and deliberate attacks to evaluate the vulnerability of the railway network, which ignored the actual geographical attributes of the railway lines. Khademi et al. proposed a post-hazard vulnerability analysis for the designed emergency transportation networks in Tehran, an earthquake-prone metropolis in a developing country [38]. Binti Sa’adin et al. highlighted flood risks imposed on the HSR (High-Speed Rail) system caused by local conditions, including topographical, geological and climatic variations along the proposed HSR route in Malaysia [39]. Yin et al. analyzed the vulnerability of a railway network in the event of earthquakes based on the theory of complex networks [11]. The above studies only considered a single geological hazard for the vulnerability analysis, but in an actual situation, the railway network is often under the joint influence of multiple geological hazards. Therefore, based on the theory of complex networks and linear reference, a geographical railway network was constructed in this paper, which retains the geographical and topological characteristics of the railway network. Then, taking the impact on overall network efficiency as the vulnerability index, combined with the hazard susceptibility model and the geological hazard data along the railways, the railway network vulnerability is analyzed under various geological hazards.

3. Materials and Methods

3.1. Materials

3.1.1. Railway Network

The train operation data used in this paper are from the CHINA RAILWAY website, which only includes mainland China. Information including the train number, type, station sequence, station, arrival time and departing time was obtained based on the railway operation chart in 2019 for more than 9000 train numbers and 3048 stations. On this basis, information including geographical coordinates and detailed addresses of each station was collected through applications such as Baidu Map and Google Map, and stored in the database, as shown in Table 1.

Table 1. An Example of Train Operation Schedule.

Train No.	Sequence	Station Name	Arrival Time	Departure Time	Stop Time (min)	Longitude	Latitude
C1001	1	Changchun	—	5:47	—	125.33	43.92
	2	Jilin	6:27	6:29	2	126.58	43.86
	3	Dunhua	7:23	7:25	2	128.25	43.39
	4	Yanji West	8:04	8:04	—	129.42	42.91

3.1.2. Influence Factors of Geological Hazards

Data of more than 250,000 historical geological hazard points such as earthquakes, collapses, landslides and debris flows were obtained from the Resource and Environment Science and Data Center. The earthquake points with a magnitude greater than 4.5 ($ms \geq 4.5$) were selected for the susceptibility calculation. The susceptibility of collapses, landslides and debris flows in the research area was studied with 15 influence factors, including elevation, slope, aspect, lithology, geology, distance to faults, distance to roads, distance to railways, distance to rivers, NDVI (Normalized Difference Vegetation Index), land cover, seismic peak ground acceleration, annual average precipitation, monthly precipitation variation coefficient and annual average ≥ 50 mm rainstorm days as the evaluation indicators on the premise of fully considering factors such as the size, scope and accuracy of the research area and the availability of relevant data. Data and sources involved in the study are listed in Table 2.

Table 2. Data Sources.

Influence Factors	Data Name	Sources
Elevation, Slope, Aspect	Geological hazards data such as earthquakes, collapses, landslides, and debris flows SRTM DEM (Shuttle Radar Topography Mission Digital Elevation Model) 90 m data	Resource and Environment Science and Data Center Geospatial Data Cloud
Lithology, Geology, Distance to faults	1:1,000,000 digital geological map data	Geoscientific Data & Discovery Publishing System
Distance to roads, Distance to railways, Distance to rivers	1:1,000,000 basic geographic information data public version (2021)	National Catalogue Service for Geographic Information
Land cover	30 m global surface cover data	National Catalogue Service for Geographic Information
NDVI	Annual 1 km NDVI spatial distribution dataset of China	Resource and Environment Data Cloud Platform
Seismic peak ground acceleration	Seismic peak ground acceleration data	Global Seismic Hazard Assessment Program
Annual average precipitation, Monthly precipitation variation coefficient, Annual average ≥ 50 mm rainstorm days	Meteorological data	National Meteorological Resources Sharing Service Platform

3.1.3. Geological Hazards along the Railway

For the geological hazards that cause actual damage to the train operation, search engines such as Baidu, Bing and Sogou were used for obtaining detailed information [40], as shown in Figure 1. First, the names of all railway lines in mainland China, such as the Beijing–Guangzhou Railway, Beijing–Kowloon Railway and Beijing–Shanghai Railway, as well as train operation status such as disruption, delay and derail were collected. Second, a combination of railway line names, train operation status and geological hazard names was used for constructing the search items, including earthquake and Beijing–Guangzhou railway line and train disruption. If the news contained any search items, we saved the title and URL of the news. Third, the data are cleaned, standardized and filtered. If the searched results have the same URL or the same title, they are considered to be duplicate, and the redundant duplicate data are deleted. Finally, the “URL”, “railway name”, “hazard type”, “occurrence time” and “occurrence location” were automatically extracted from the results, and the obtained geological hazards were spatialized and stored in the database according to the types of geological hazards.

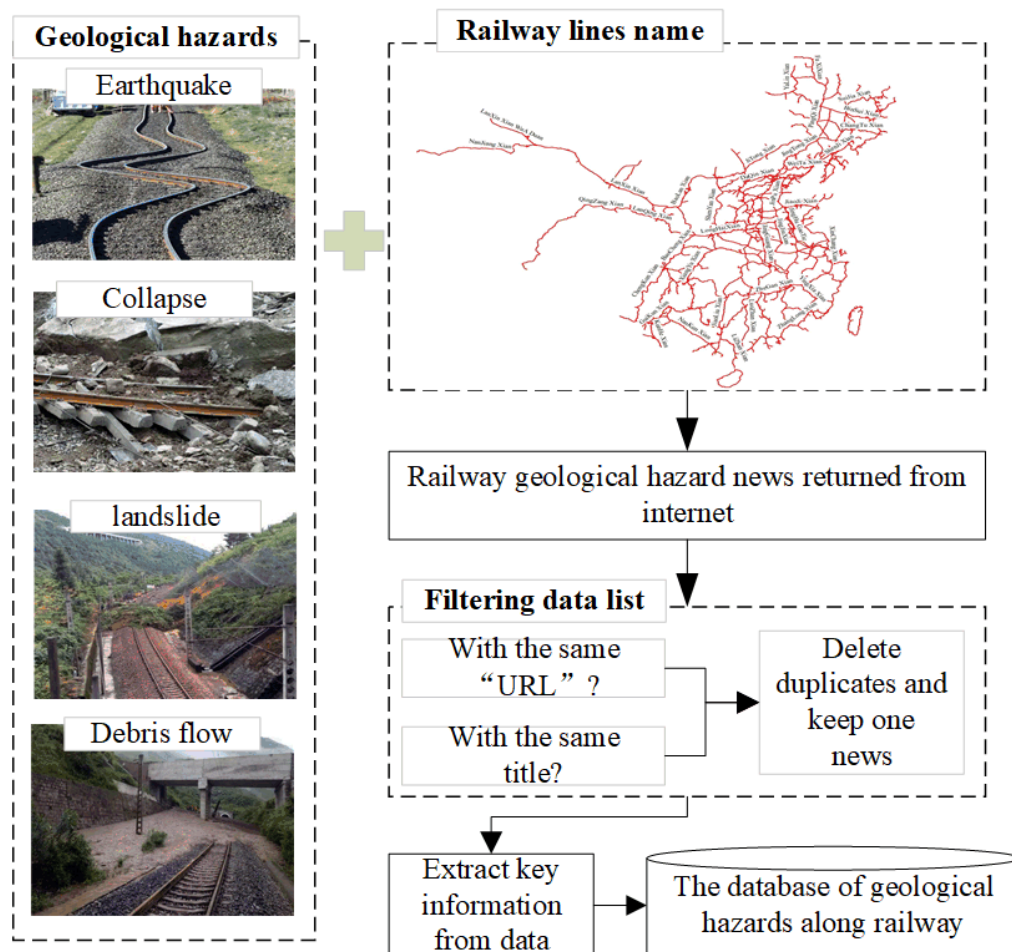


Figure 1. Obtaining Process of the Geological Hazard Data Along the Railway.

3.2. Geographical Railway Network Modeling

A railway network is composed of stations and railway lines and a railway line covers a few stations. The complex network, in general, is simplified as per the actual situation to reduce the modeling cost of network topology and improve the efficiency of network analysis. In that case, the following assumptions are made in the modeling of the railway network topology. First, the railway network topology is modeled based on the existing normal-speed railway network and high-speed railway network, with the existing operating lines considered. Second, the railway network is abstracted as an undirected network in the modeling of railway network topology, ignoring the directionality of railway transportation. Third, the railway network is abstracted into a weighted or unweighted network, and whether the influence of weights should be considered is determined as per the research based on the actual operation of the railway network. The edge weight between stations, that is, the number of trains passing between station pairs, is considered due to the limitation of relevant data. Thus, the influence of the point weight of the station is ignored.

The commonly used modeling methods of railway complex networks mainly include Space L and Space P. Space L regards railway stations as the nodes, and there is an edge between any two consecutive nodes on its route. Space P regards railway stations as the nodes, where there is an edge between both nodes on the route [41,42]. According to the actual operation status of the railway network that stations are linked by the rail tracks, if the rail tracks between certain two stations are cut, the connectivity on the operation line will be suspended into two halves at the cutting point, and the link between the stations is broken. Therefore, this paper established a geographical railway network with Space L model, which regards all the passing stations of a train as nodes, and there is an edge between adjacent stations on the same train line.

In a complex network model, the geographical railway network is abstracted as a graph $G = (V, E)$ composed of a point set V and an edge set E , in which set V is the element of the railway station, $V = \{1, 2, 3, \dots, i, \dots, n\}$, set E consists of the edges of any two stations in the railway network, $E = \{\delta_{ij}\}$, δ_{ij} indicates the connection relationship between stations i and j , $\delta_{ij} = 1$ indicates that station i has a connection with station j , $\delta_{ij} = 0$ indicates station i has no connection with station j [5]. On this basis, combining the stations the train passes, the mileage position of the station on the line and the type of train, the train operation process is mapped to the actual railway line using linear referencing technology to obtain the final geographical railway network, as shown in Figure 2. The specific method of mapping the point pair of the complex network model to the actual railway line is shown in Figure 3. First, if there is only one line connecting the station node pair, then the mileage position of the station node pair on the line can be directly calculated, as shown in Figure 3a. Second, if there is one extra line connecting the station node pair, then the line corresponding to the station node can be determined according to the type of train and the lines of the previous and next station, as shown in Figure 3b. Third, if there is no corresponding line passing between the station node pair, the intermediate node station between the stations is determined according to the shortest-path principle based on the second principle, and the original Start Station–End Station node pair is transformed into Start Station–New Station and New Station–End Station node pairs, as shown in Figure 3c.

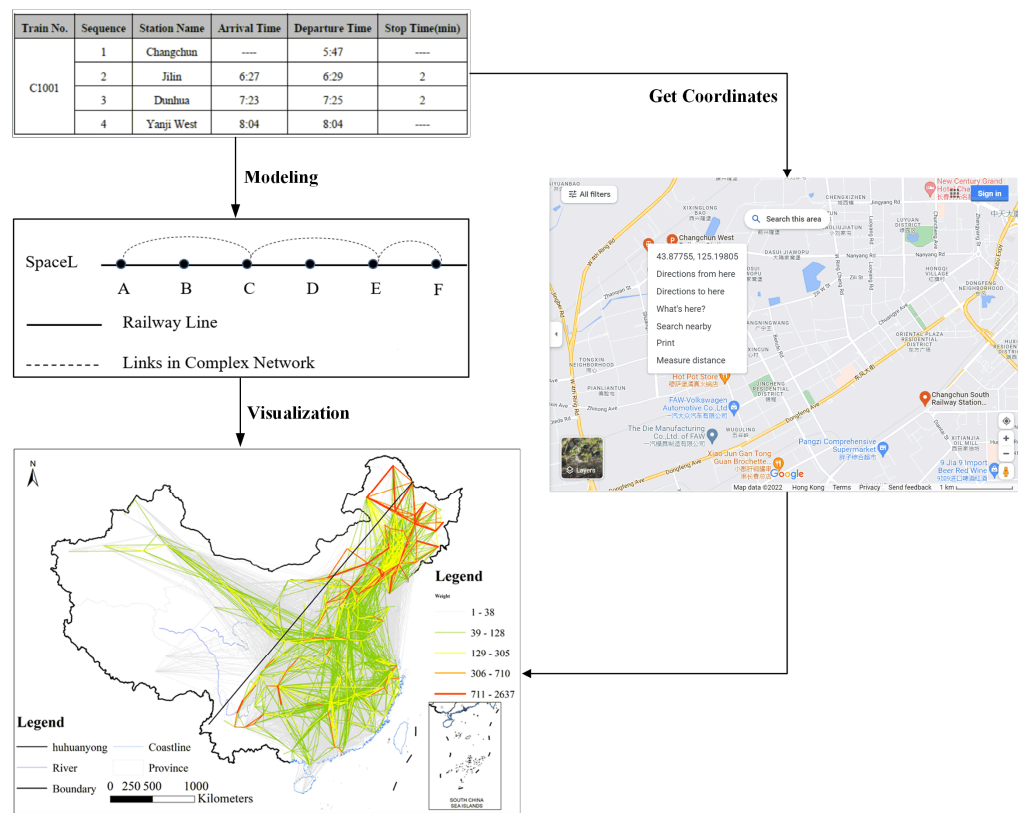


Figure 2. Geographical Railway Network Modeling.

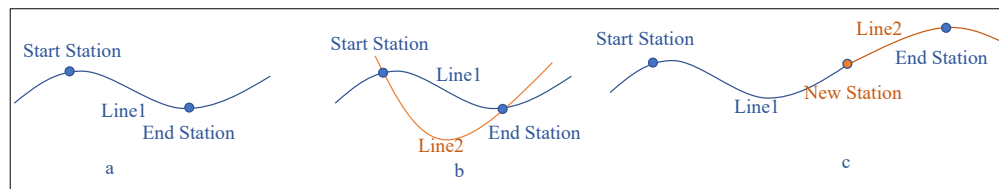


Figure 3. Line Information of the Station: (a) Only One Line Connects the Station Node Pair; (b) More than One Lines Connects the Station Node Pair; (c) No Corresponding Line Passes between the Station Node Pair.

3.3. Vulnerability Evaluation of Geographical Railway Network under Geological Hazards

Geological hazards along China's railway are of wide distribution, high frequency and so severe that they have affected and threatened the regular operation and traffic safety of railways. Among these geological hazards, earthquakes, collapses, landslides and debris flows are the major types [43]. The hazard-stricken railway sections have accounted for over 20% of the total running mileage, and many other lines are at risk of geological hazards [2,17]. Therefore, the typical geological hazards of earthquakes, collapses, landslides and debris flows were chosen to carry out the vulnerability analysis on China's geographical railway network. The mechanism of geological hazards is not included, only the failures of nodes and edges in the railway network system caused by hazards are studied, as well as the vulnerability of the entire railway system which is further studied based on this. In this way, it is conducive to focusing the research on the characteristics of the system itself [44]. To begin with, the areas that are vulnerable to geological hazards in the geographic railway network were obtained from the evaluation of the susceptibility of typical geological hazards. Next, the vulnerability section was acquired from the calculation of the actual number of hazards and the susceptibility of the railway network in the area. Meanwhile, the railway lines and operating train data in the above-mentioned vulnerability section were counted. At last, the efficiency changes in the whole

geographic railway network were analyzed to evaluate the station nodes of the geographic railway network under typical geological hazard conditions by means of removing each station node successively with the global network efficiency as an indicator. On this basis, the stations featuring greater vulnerability were considered as key protection objects.

3.3.1. Susceptibility Evaluation of Geological Hazards

Susceptibility evaluation of geological hazards is to predict the future possibility of generating geological hazards in the area after determining the spatial probability of occurrence of geological hazards under certain hazard-pregnancy backgrounds with no consideration of the specific time and scale of occurrence [45]. Earthquakes are when the collapse of ground buildings, traffic interruptions and the destruction of other lifeline engineering facilities within a certain range are caused by an earthquake wave from the rupture of the earth's internal medium (rock) triggered by sudden and rapid movement under the effect of force [46]. Development and distribution characteristics of geological hazards such as collapses, landslides and debris flows are subject to factors such as surface terrain, geological structure, vegetation coverage and precipitation [43]. Hence, this paper discussed the approach to evaluating hazard susceptibility from the perspective of the causes of geological hazards.

1. Susceptibility evaluation of earthquakes

In general, the seismicity level in an area is consistent within a certain time scale since the geological structure is changed slightly in a short time scale (<100a) [46]. In a large regional scale, the higher the frequency of earthquakes in a certain area in history, the greater the possibility of earthquakes in the future [47]. Earthquakes can be abstracted as “point” accidents in space from the perspective of spatial analysis [48]. Kernel density analysis can quantitatively analyze the occurrence probability of hazard points in different geographic spatial locations based on the earthquakes that have occurred. The higher the kernel density value, the greater the probability of hazard occurrence and the denser the form of hazard points, and vice versa [49]. The kernel density calculation equation is as follows:

$$KDE(x) = \frac{1}{nh} \sum_{i=1}^n K\left(\frac{x - x_i}{h}\right) \quad (1)$$

where, $KDE(x)$ is the kernel function, h is the search radius, n is the number of points in the searching area and $x - x_i$ is the distance from the estimated point x to the sample point x_i .

2. Susceptibility evaluation of collapses, landslides and debris flows

Geological hazards such as collapses, landslides and debris flows are influenced by a variety of factors that have varying magnitudes and natures in different geological environments [50,51] and there is an “optimized factor combination” contributing the most to the occurrence of geological hazards [52–54]. The susceptibility evaluation of geological hazards based on the information value model is to convert the measured values of various impact factors known to affect regional stability into information values that reflect regional stability through the information provided by the areas where geological hazards occurred. More precisely, the closeness of the relationship between the influence factor and the research object is evaluated using the information value. The greater the information value, the higher the possibility of geological hazards occurring. The information value can be expressed as [55–57]:

$$I_i = \log_2 \frac{N_i/N}{S_i/S} \quad (2)$$

where, I_i is the amount of information value provided by the influence factor x_i on the possibility of geological hazards, N_i is the number of grid cells of geological hazards occurring in a specific category of the influence factor x_i , S_i is the number of grid cells in a specific category of the influence factor x_i , N is the number of grid cells of hazards occurring in the research area, and S is the total number of grid cells in the research area.

The total information value of various evaluation units can be calculated by adding information values of various influence factors.

$$I = \sum_{i=1}^n I_i = \sum_{i=1}^n \log_2 \frac{N_i/N}{S_i/S} \quad (3)$$

where, I is the gross information value in the evaluation unit, and the possibility of geological hazards is on the rise with the increasing I value. The greater the I value, the higher the susceptibility to geological hazards.

3. Susceptibility evaluation of integrated geological hazards

On the basis of calculating the susceptibility value for a single geological hazard, the kernel density of the integrated geological hazards is calculated according to the ratio of the number of times different geological hazards occur along the railway, which is regarded as the susceptibility of the integrated geological hazards. The calculation equation is as follows:

$$F = \frac{f_j}{\sum f_j * I_j} \quad (4)$$

where, f_j is the number of times different geological hazards occur along the railway and I_j is the susceptibility value of the corresponding geological hazard.

3.3.2. Vulnerability Evaluation of Geographical Railway Network

If there are more geological hazards in a certain area, but the railways are damaged less frequently, it is considered that the railways in the area have a stronger resistance to geological hazards. On the contrary, the railways in this area are considered to have weaker resistance to geological hazards. Therefore, this paper used the geological hazard susceptibility and the number of rail tracks damaged in geological hazards to measure the vulnerability of the railway network. First, the railway line is divided into sections according to a certain distance, and the number of geological hazards in each section is calculated. Then, the susceptibility of geological hazards is mapped to the railway line through spatial overlay, and the vulnerability in each railway section is calculated by Equation (5). The equation for calculating the vulnerability of the railway section is as follows:

$$V_l = \frac{E_l}{F_l} \quad (5)$$

where, V_l means the vulnerability of the railway section, E_l is the number of geological hazards that occurred in the railway section and F_l represents the maximum susceptibility value of geological hazards in the railway section.

Moreover, the station node is an important part of the geographic railway network for it is a gathering place for passenger flows and train operation. Regarding the station node in the railway vulnerability section, the vulnerability of each station in the railway geographic network under geological hazard conditions was analyzed with the overall network efficiency as the main indicator of network vulnerability analysis. The network efficiency was represented by the mean of the reciprocal sum of node distances in the geographic railway network. Further, the station node vulnerability of the railway geographic network was evaluated through statistically analyzing the change in the overall network efficiency after the sequential removal of each station node. Then, key points in the railway geographic network are selected as the protection objects according to the results of the network vulnerability analysis. The calculation can be performed as follows [58]:

$$\begin{aligned} E_{global} &= \frac{1}{N(N-1)} \sum_{i \neq j} \frac{1}{d_{ij}} \\ V_i &= \frac{E_{global} - E'_{global}}{E_{global}} \end{aligned} \quad (6)$$

where, E_{global} is the overall network efficiency, N is the number of nodes in the network, d_{ij} is the shortest distance between node i and node j , V_i represents the importance of the station and E'_{global} is the overall network efficiency upon the removal of the station i .

4. Results and Analysis

4.1. Spatial Distribution Analysis of Geographical Railway Network

On the basis of modeling the railway topological network according to the complex network theory, the geographical railway network can be obtained by mapping the railway topological network to the actual railway line through the station, so the number of trains in each section of each railway line can be obtained, as shown in Figure 4. The busiest railway operation sections are basically located to the east of the Hu Huanyong Line, mainly distributed along the “eight verticals and eight horizontals”. The busiest area includes the vertical Beijing–Shanghai High-Speed Railway, Beijing–Guangzhou High-Speed Railway and Beijing–Harbin High-Speed Railway, followed by the horizontal Xuzhou–Lanzhou High-Speed Railway, Shanghai–Kunming High-Speed Railway, Fuzhou–Xiamen–Zhangzhou High-Speed Railway and Chengdu–Chongqing High-Speed Railway. The railways to the west of the Hu Huanyong Line are generally not particularly busy. As an important part of the railway network in Northwest China, the Lanzhou–Xinjiang Railway is the line with the most train-passing points.

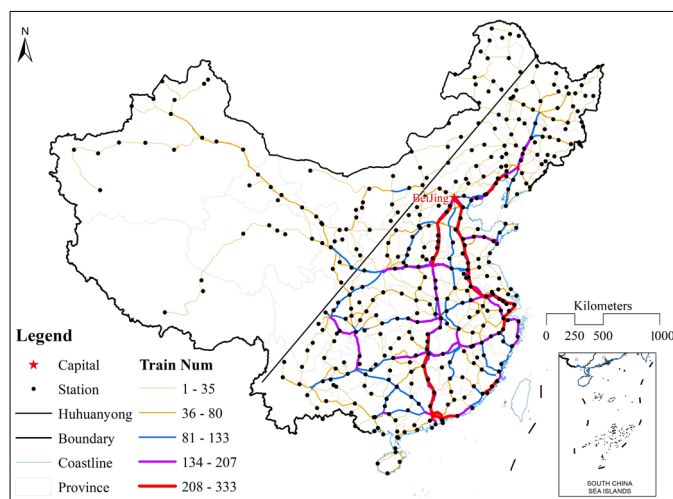


Figure 4. The Number of Train-Passing Points on the Railway Lines.

4.2. Time–Space Analysis of Geological Hazards along the Railway

Figure 5 is the proportional distribution of geological hazards along the railway, with earthquakes accounting for 48%, landslides accounting for 28%, debris flows for 17% and collapses for 7%. The earthquake is the most influential geological hazard to the railway, followed by landslide and debris flow, while collapses have the least significant impact on the railway. This is because China is located at the intersection of the world's two major seismic belts, with intense crustal tectonic activities, as well as frequent, strong and wide distributed seismic activities. Frequent strong vibrations break and loosen the rocks and bring about material conditions for the occurrence of hazards at the same time.

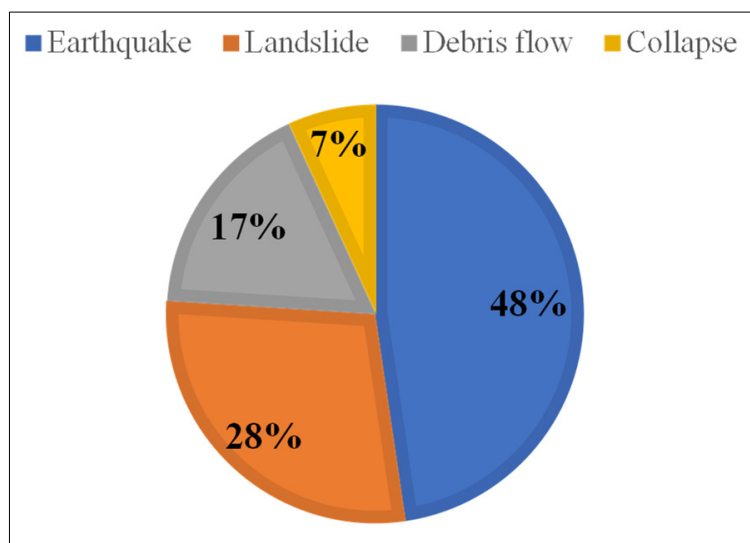


Figure 5. Proportional Distribution of Railway Geological Hazards.

Figure 6a is the inter-annual frequency statistics of railway disastrous accidents caused by geological hazards, and the frequency of geological hazards along the railway has shown an upward trend over the years. The geological hazards along the railway have increased significantly in the 2010–2021 period, which may be caused by the increased railway network coverage and higher frequency of extreme weather. Figure 6b provides the statistics on the monthly frequency of geological hazards along the railway. The geological hazards along the railway mainly happen in June, July and August, with a significant concentration. The main reason is that the occurrence of geological hazards along the railway is closely related to precipitation. China is in the monsoon region, with concentrated precipitation and rainstorms in summer. The precipitation in summer accounts for 56.5% of the national average annual precipitation [59]. Continuous rainfall and rainstorms have caused large-scale and frequent geological hazards in weak strata, unstable slopes and loosely structured gully areas, so as to trigger disastrous railway accidents.

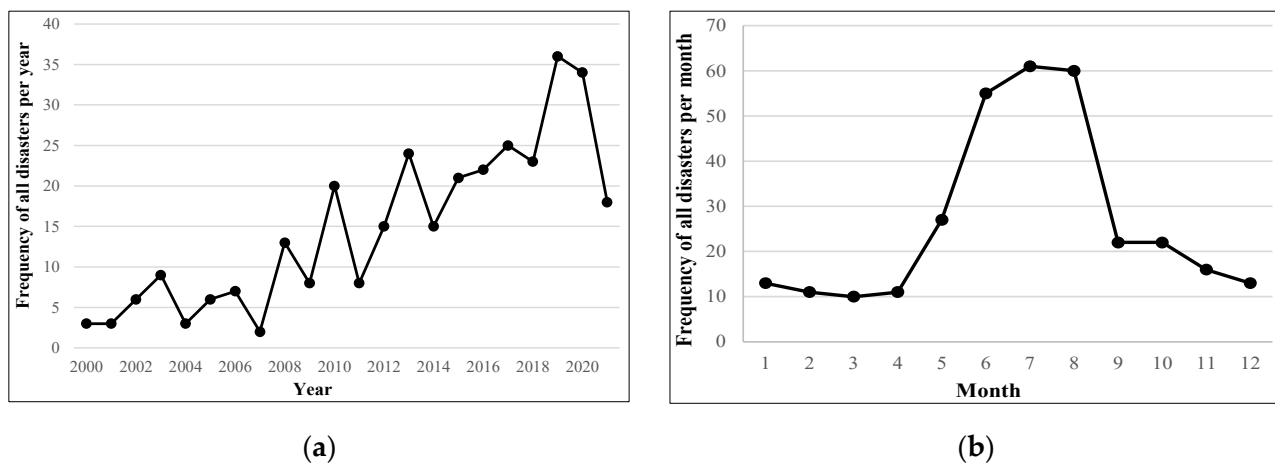


Figure 6. Frequency Statistics of Geological Hazards along the Railway: (a) Inter-Annual Frequency Statistics of Geological Hazards along the Railway; (b) Statistics on the Monthly Frequency of Geological Hazards along the Railway.

Figure 7 is the spatial distribution of geological hazards along the railway. Earthquake-caused disastrous accidents are mainly in the western and southwestern provinces and autonomous regions, such as Sichuan, Xinjiang, Yunnan and Guangxi, where strong earthquakes occur frequently, and there are high mountains and broken rocks, which are prone to the occurrence of earthquake hazards along the railway. The affected lines include Chengdu–Kunming Railway, Lanzhou–Xinjiang Railway, Southern Xinjiang Railway and Chengdu–Chongqing Railway. Collapse-caused disastrous accidents are mainly in the provinces of Jiangxi, Guangdong and Huanan, and the affected lines include Beijing–Kowloon Railway, Jiaozuo–Liuzhou Railway and Chongqing–Huaihua Railway. Landslide-caused disastrous accidents are mainly in Chongqing and the provinces of Guizhou, Gansu and Sichuan, and the affected lines include Shanghai–Kunming Railway, Chongqing–Guiyang Railway, Chongqing–Huaihua Railway and Lanzhou–Lianyungang Railway. Debris-flow-caused disastrous accidents are mainly in the provinces of Shaanxi, Xinjiang, Sichuan and Guizhou, and the affected lines include Baoji–Chengdu Railway, Nanning–Kunming Railway and Lanzhou–Xinjiang Railway.

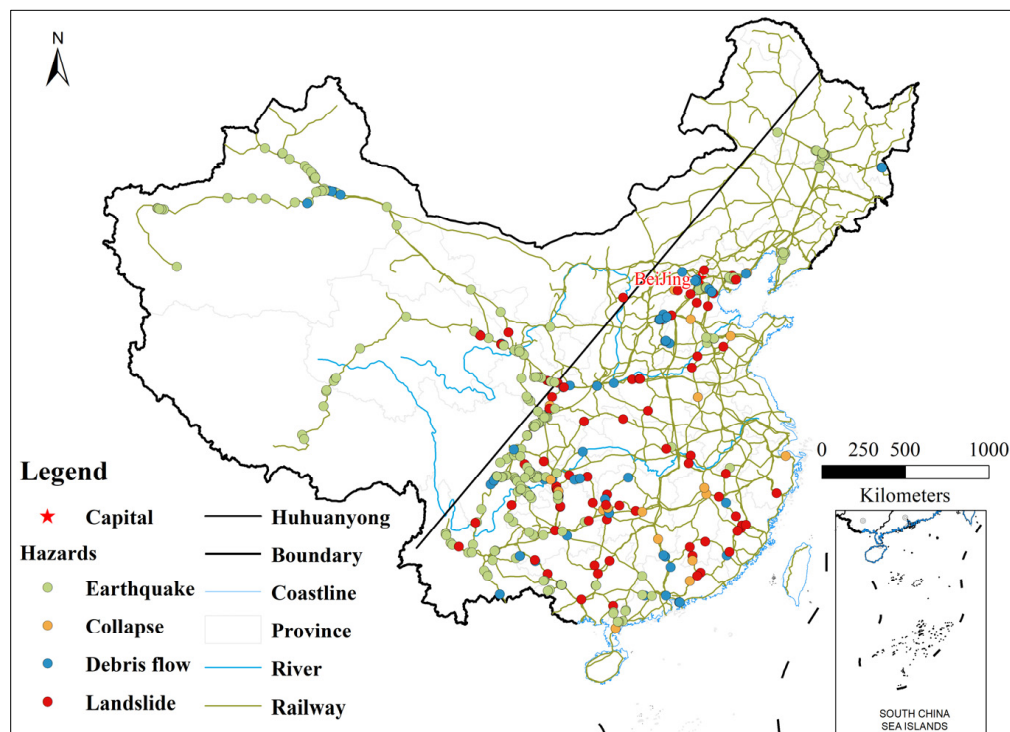


Figure 7. Spatial Distribution of the Railway Geological Disastrous Accidents.

4.3. Susceptibility Analysis of Geological Hazards

The influence factor data were converted into $1 \text{ km} \times 1 \text{ km}$ raster data through processing, such as spatial interpolation, reclassification and feature to raster. On this basis, the values of the influence factors are classified, as shown in Figure 8.

The susceptibility of collapses, landslides and debris flows is evaluated using the information value method. First, each layer of influence factors is overlaid with the obtained geological hazard points to obtain the number and area of geological hazards occurring under each level of classification. Then, the information value of each factor classification value is calculated from Equation (2), as shown in Table 3.

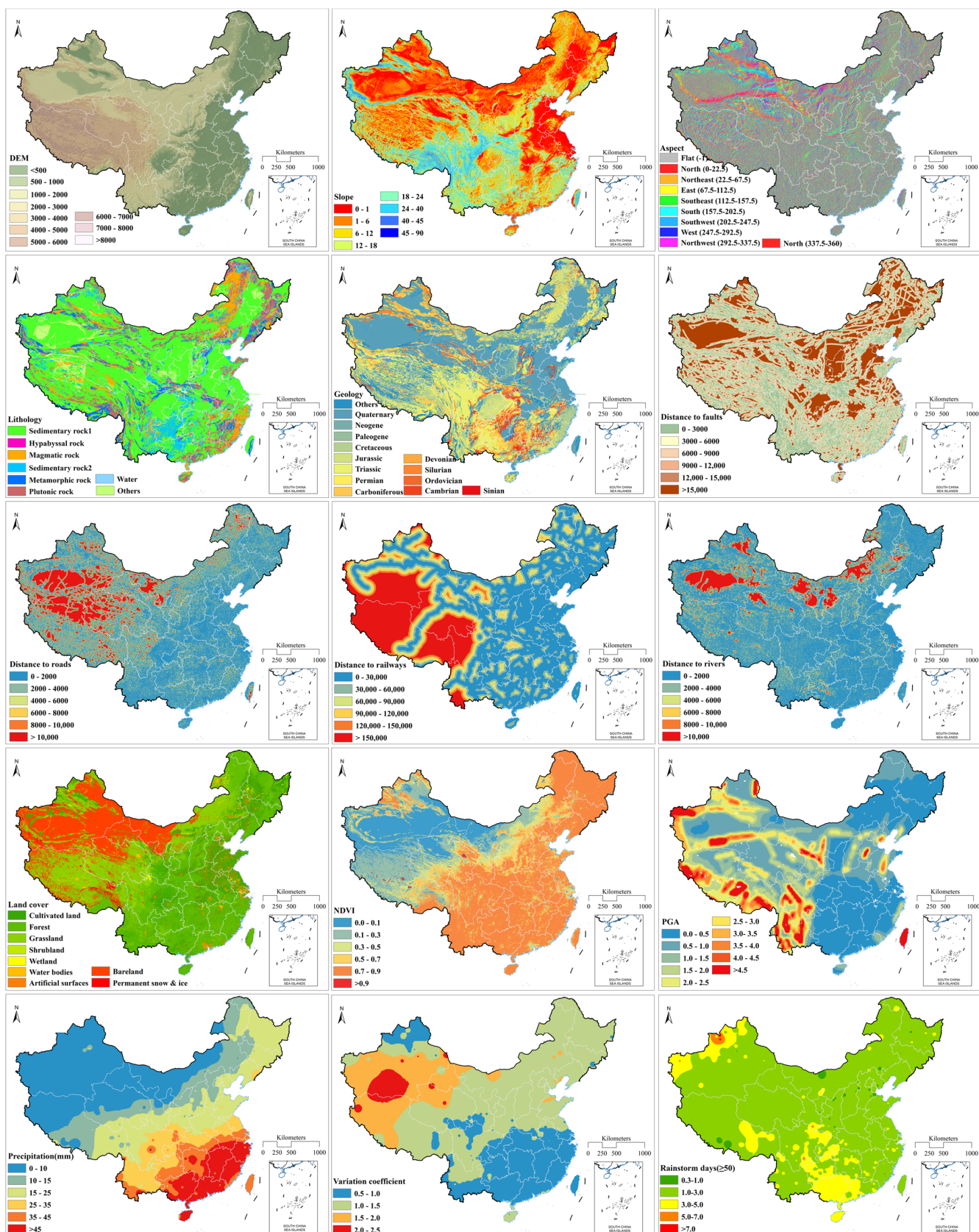


Figure 8. Characteristics of Influence Factors.

Table 3. The Information Values of Influence Factors.

Influence Factors	Classification	Information Value (Collapse)	Information Value (Landslide)	Information Value (Debris Flow)	Influence Factors	Classification	Information Value (Collapse)	Information Value (Landslide)	Information Value (Debris Flow)
DEM	<500	0.65	0.56	-0.52	Slope	0–1	-1.24	-2.10	-1.84
	500–1000	0.08	0.39	-0.23		1–6	-0.14	-0.38	-0.43
	1000–2000	-0.27	-0.18	0.15		6–12	0.44	0.51	0.31
	2000–3000	-0.02	-0.03	1.00		12–18	0.46	0.65	0.52
	3000–4000	-0.80	-1.56	0.67		18–24	0.31	0.61	0.54
	4000–5000	-1.68	-2.95	0.03		24–40	0.23	0.29	0.71
	5000–6000	-4.04	-4.87	-2.85		40–45	0.60	0.09	0.89
	6000–7000	0.00	0.00	0.00		45–90	0.42	-0.21	0.44
	7000–8000	0.00	0.00	0.00		others	-0.21	-0.47	-0.47
	>8000	0.00	0.00	0.00		Sedimentary rock1	-0.20	-0.07	-0.18
Aspect	-1	-0.43	-0.49	-0.55	Lithology	Hypabyssal rock	0.37	0.31	0.41
	0–22.5, 337.5–360	-0.06	-0.08	-0.12		Magmatic rock	-0.17	0.19	0.22
	22.5–67.5	0.01	-0.01	0.08		Sedimentary rock2	0.34	0.15	0.13
	67.5–112.5	0.13	0.15	0.26		Metamorphic rock	0.26	0.39	0.68
	112.5–157.5	0.17	0.19	0.30		Plutonic rock	0.53	0.04	0.21
	157.5–202.5	0.11	0.06	0.22		Water	-0.76	-0.45	-1.34
	202.5–247.5	0.00	-0.05	-0.05		0–3000	0.19	0.29	0.44
	247.5–292.5	-0.15	-0.09	-0.39		3000–6000	0.10	0.08	0.09
	292.5–337.5	-0.17	-0.12	-0.49		6000–9000	-0.04	-0.09	-0.08
	others	0.17	0.10	0.66		9000–12,000	-0.18	-0.24	-0.28
Geology	Quaternary	-0.97	-1.25	-0.73	Distance to railways	12,000–15,000	-0.31	-0.31	-0.43
	Neogene	-0.97	-0.93	-0.43		>15,000	-0.28	-0.46	-1.06
	Paleogene	-2.07	-1.43	0.56		0–2000	0.45	0.42	0.45
	Cretaceous	0.10	0.47	0.01		2000–4000	-0.32	-0.14	-0.40
	Jurassic	0.72	0.50	0.14		4000–6000	-0.80	-0.67	-0.65
	Triassic	-0.11	0.21	0.54		6000–8000	-1.39	-1.77	-1.21
	Permian	-0.04	0.25	-0.03		8000–10,000	-1.93	-3.33	-1.90
	Carboniferous	0.23	-0.38	-0.50		>10,000	-3.41	-5.60	-2.98
	Devonian	0.60	0.46	0.33		0–30,000	0.37	0.34	0.12
	Silurian	0.61	1.02	0.28		30,000–60,000	0.15	0.29	0.09
Distance to rivers	Orдовician	0.46	0.42	0.17	Land cover	60,000–90,000	-0.14	-0.08	-0.01
	Cambrian	0.87	0.98	0.12		90,000–120,000	-1.12	-0.66	-0.17
	Sinian	1.45	1.32	0.75		120,000–150,000	-1.26	-1.18	-0.16
	0–2000	0.25	0.24	0.27		>150,000	-1.58	-2.28	-0.34
	2000–4000	-0.36	-0.18	-0.49		Cultivated Land	0.38	0.45	0.08
	4000–6000	-0.74	-0.85	-0.59		Forest	0.60	0.78	0.28
>10,000	6000–8000	-0.93	-1.77	-1.10	Wetland	Grassland	-0.47	-0.77	0.25
	8000–10,000	-1.32	-2.77	-1.57		Shrubland	-0.18	-0.21	0.44
	>10,000	-3.34	-7.83	-3.67		Wetland	-1.15	-2.20	-0.88

Table 3. *Cont.*

Influence Factors	Classification	Information Value (Collapse)	Information Value (Landslide)	Information Value (Debris Flow)	Influence Factors	Classification	Information Value (Collapse)	Information Value (Landslide)	Information Value (Debris Flow)
NDVI	0–0.1	−2.13	−5.51	−1.98	PGA	Water Bodies	0.00	−0.10	−0.36
	0.1–0.3	−1.20	−3.49	−0.59		Artificial Surfaces	0.47	0.04	0.00
	0.3–0.5	−0.35	−1.32	0.31		Bareland	−1.71	−4.28	−1.29
	0.5–0.7	0.23	−0.14	0.54		Permanent Snow &Ice	−3.06	−4.55	−2.37
	0.7–0.9	0.42	0.61	0.19		0.0–0.5	0.49	0.71	−0.62
	>0.9	−4.13	−4.46	−2.87		0.5–1.0	−0.61	−1.38	−0.53
	0–10	−1.06	−2.36	−0.68		1.0–1.5	−0.03	−0.66	0.24
	10–15	−0.92	−1.36	0.46		1.5–2.0	−0.30	−0.36	0.34
	15–25	−0.34	−0.83	0.28		2.0–2.5	−0.24	−0.40	0.43
	25–35	0.71	1.04	0.56		2.5–3.0	−0.18	−0.36	0.57
Precipitation	35–45	0.09	0.85	−0.75		3.0–3.5	−0.35	−0.56	0.62
	>45	1.44	1.46	−0.24		3.5–4.0	−0.50	−0.42	0.62
	0.3–1.0	−0.79	−0.77	1.86		4.0–4.5	−0.53	−0.30	0.66
	1.0–3.0	−0.20	−0.11	−0.04		>4.5	−0.63	−0.24	0.66
	3.0–5.0	0.74	0.49	−0.03	Variation	0.5–1.0	0.81	1.02	−0.26
	5.0–7.0	0.51	0.17	0.05		1.0–1.5	−0.33	−0.60	0.32
Rainstorm days	>7.0	0.15	0.00	−1.48		1.5–2.0	−1.60	−4.14	−0.92
						2.0–2.5	−0.90	−3.41	−0.77

The obtained information values of the influence factors are assigned to the respective susceptibility factor layers to be the pixel value of each factor. Then, the total information value is calculated by adding up each factor layer through Equation (3), and the research area is divided by information value into five levels through using the natural breakpoint method, as shown in Figure 9. The areas with high susceptibility to collapses are approaching those areas with high susceptibility to landslides, which are located in Southeast and Southwest China. Most of the areas with high susceptibility to debris flows are in Southwest, North and Northeast China. This is because it has large terrain undulations, well-developed gullies, deep valleys and steep slopes in the southwestern mountainous area, where geological hazards are easily caused by the heavy rainfall. In the southeastern area, due to an increase in disastrous weather, such as typhoons, tropical storms and storm surges, sudden geological hazards in low hilly areas have shown an increasing trend. The susceptibility of earthquakes is estimated by kernel density, which is calculated based on historical earthquake locations. The denser the aggregation morphology, the greater the probability of the hazard occurrence. There are small areas with high susceptibility to earthquakes, as the vast majority of earthquake belts in China are located in the southwest and northwest regions.

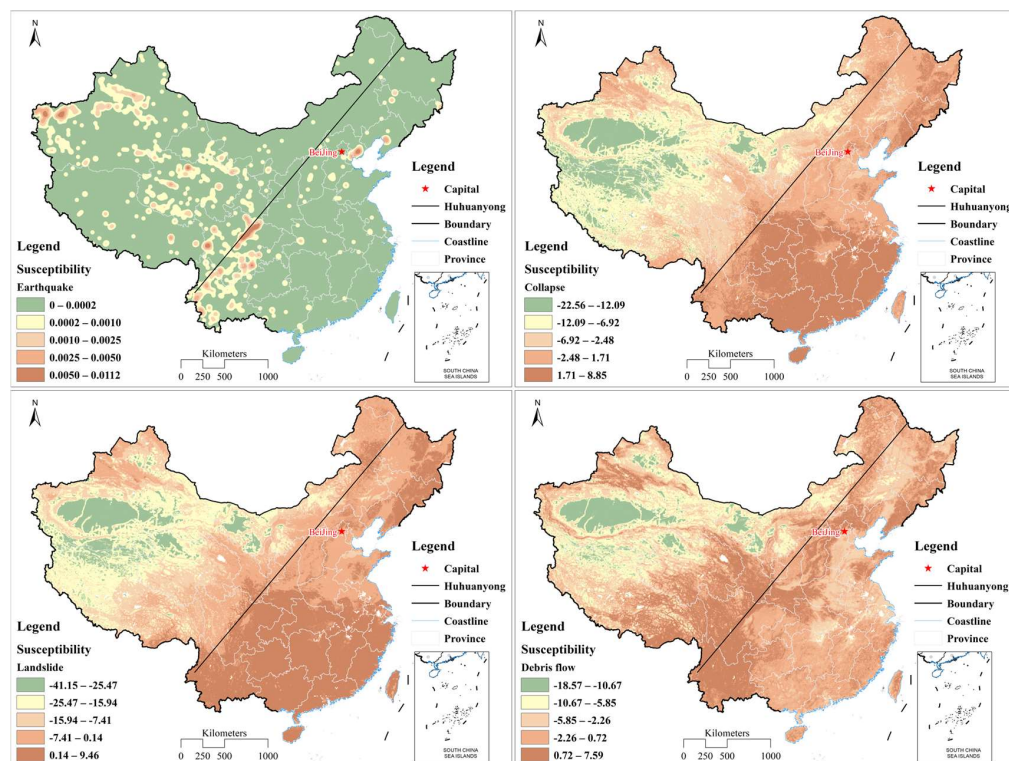


Figure 9. Evaluation Analysis of Susceptibility to a Single Geological Hazard.

The receiver operating characteristic (ROC) curve is adopted to evaluate the precision of susceptibility model of collapses, landslides and debris flows, as shown in Figure 10. The Y axis of the ROC curve represents the true-positive rate (sensitivity), which is the cumulative percentage of real geological hazards' area in each susceptibility level; the X axis of the ROC curve represents the false-positive rate (specificity), which is the cumulative percentage of susceptibility area in each susceptibility level in the research area [60,61]. AUC (Area Under the Curve) value is the area enclosed by the ROC curve and X axis, which is used to measure the accuracy of modeling results. The larger the AUC value, the higher the precision of the results. The AUC values of collapses, landslides and debris flows susceptibility models are 0.80, 0.86 and 0.816, respectively, indicating that the evaluation model has high accuracy and can be applied to the evaluate geological hazard susceptibility.

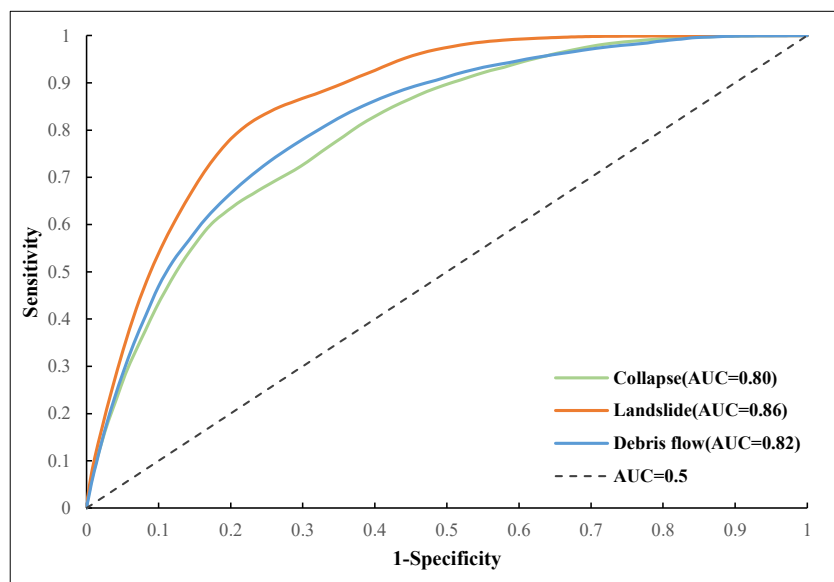


Figure 10. ROC Curve of Susceptibility to Geological Hazards.

The susceptibility of integrated geological hazards can be calculated from Equation (4) on the basis of susceptibility to a single hazard, which is divided into five grades, as shown in Figure 11. Evidently, 4% of the railway lines in the geographic railway network are located in the areas with high susceptibility (V grade) to geological hazards, including Baoji–Chengdu Railway, Xi'an–Chengdu High-Speed Railway, Neijiang–Liupanshui Railway and Chengdu–Chongqing Railway in Southwest China, Beijing–Harbin Railway, Shenyang–Dalian Railway and Tianjin–Shanhaiguan Railway in Northeast China, and Southern Xinjiang Railway in Northwest China. In addition, 26% of the lines are exposed in the areas with grade IV susceptibility to geological hazards, which are distributed mostly in Southwest, Northwest and Northeast China. Therefore, geological hazards should be avoided with corresponding protective measures established in these areas during railway construction.

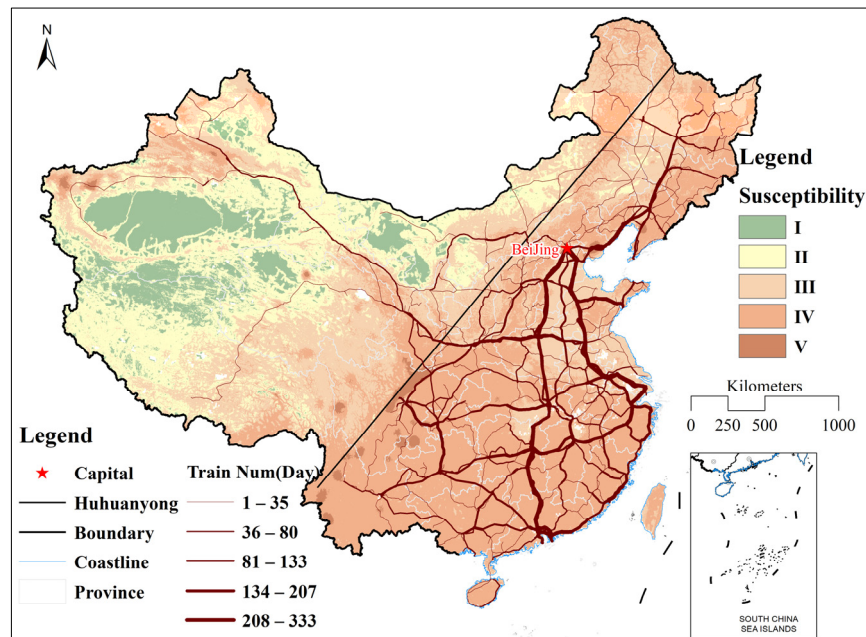


Figure 11. Distribution of Susceptibility to Integrated Geological Hazards.

4.4. Vulnerability Analysis of Geographical Railway Network

First, the number of hazards occurring in each section was counted after the geological hazard points along the railway line were mapped to the railway section. Then, the spatial distribution of vulnerability to each railway line section was calculated using Equation (5) and overlaid on the geographic railway network to obtain the number of trains affected in each section, as shown in Figure 12. The railway line sections with greater vulnerability are mostly distributed in Southwest, Northwest and Northeast China, and the railway lines and sections with the greatest vulnerability are given in Table 4. To be specific, these are the Qiezixi–Honghuayuan section of Chongqing–Guizhou Railway Line, the Ebian–Xide section of Chengdu–Kunming line, and the Leshan–Yibin west section of Chengdu–Guizhou High-Speed Railway in Southwest China, with the Urumqi–Shanshan section of Lanzhou–Xinjiang Railway and the Heshuo–Yuergou section of Southern Xinjiang Railway in Northwest China, and the Harbin–Wopu section of Beijing–Harbin Railway in Northeast China and the Harbin–Shangjia section of Harbin–Manzhouli Railway. Of these, the Harbin–Wopu section of Beijing–Harbin Railway Line witnessed the most vehicles, with 109 passing vehicles, followed by the Taiyuan–Shijiazhuang section of Shijiazhuang–Taiyuan Railway, with 99 passing vehicles. Normal-speed railways, in most cases, are the most vulnerable railways due to the long construction time, incomplete infrastructure, emergency facilities as well as resources, poor emergency response capacities and small radiation ranges.

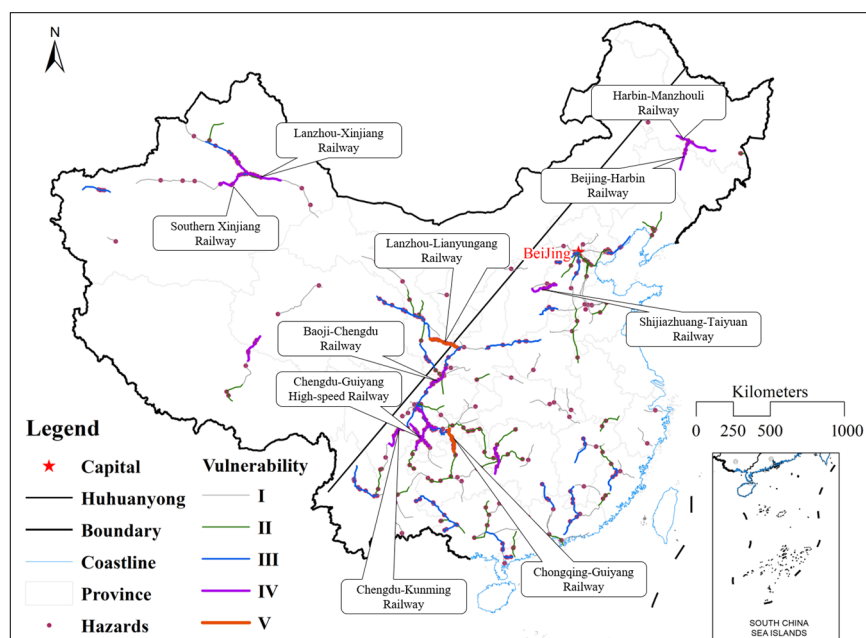


Figure 12. Vulnerability Analysis of Railways Under the Integrated Geological Hazards.

As geological hazards have varying influences on the railway network in China, the railway stations in the section with high vulnerability (grade IV and V) were deleted together with the edges adjacent to the stations. Then, the influence of the station on the overall network efficiency was calculated with Equation (6). More specifically, the station with the greatest influence on the railway network is presented in Table 5. The safe operation of the railway network will be affected directly in case of a sudden geological hazard. In such a context, professional railway rescue materials should be arranged with supporting emergency service facilities at those stations with high vulnerability to geological hazards, which can be used for rescue in case of emergencies, enhancing the response capability of the emergency management system. In this way, the safety of the railway passenger transport network in China can be guaranteed.

Table 4. The Most Vulnerable Sections in the Railway Lines.

No.	Railway	Segment	Train Number (Day)	Type	V_l
1	Chongqing–Guizhou Railway	Qiezixi–Honghuayuan	2	Normal-Speed	4.5
2	Lanzhou–Lianyungang Railway	Tianshui–Hejiadian	74	Normal-Speed	4.0
3	Chengdu–Kunming Railway	Ebian–Xide	15	Normal-Speed	2.7
4	Chengdu–Guizhou High-Speed Railway	Leshan–Yibin West	30	High-Speed	2.6
5	Beijing–Harbin Railway	Harbin–Wopu	109	Normal-Speed	2.3
6	Harbin–Manzhouli Railway	Harbin–Shangjia	51	Normal-Speed	2.3
7	Baoji–Chengdu Railway	Yangpingguan–Jiangyoubei	32	Normal-Speed	2.2
8	Shijiazhuang–Taiyuan Railway	Taiyuan–Shijiazhuang	99	Normal-Speed	2.2
9	Lanzhou–Xinjiang Railway	Urumqi–Shanshan	66	Normal-Speed	2.0
10	Southern Xinjiang Railway	Heshuo–Yu’ergou	34	Normal-Speed	1.9

Table 5. Important stations in the geological railway network.

No.	Station	V_i	No.	Station	V_i
1	Harbin	0.0239	11	Chengdu East	0.0039
2	Xining	0.0150	12	Zhenzi Street	0.0038
3	Qilongxing	0.0061	13	Harbin North	0.0036
4	Minfusi	0.0055	14	Taiyuan	0.0036
5	Xiaba	0.0050	15	Yuci	0.0034
6	Taiyuan South	0.0049	16	Ganshui	0.0034
7	Qijiang	0.0046	17	Neijiang	0.0034
8	Huaihua	0.0043	18	Shijiazhuang North	0.0032
9	Sanjiang	0.0041	19	Shimenkan	0.0031
10	Guangyuan	0.0041	20	Muzhuhe	0.0028

5. Conclusions and Future Works

In view of the existing problems of using only random attacks and deliberate attacks to analyze the vulnerability of the railway network and ignoring the joint impact of multiple hazards on the vulnerability assessment of the railway lines in the current research, this paper carried out analysis and research on the vulnerability of the geographical railway network under actual geological hazards. First, a geographic railway network was built using the complex network theory to analyze the number of trains running on the line of the actual geographic network and changes in space. It can be observed that trains passing by the railway lines of eight vertical railways and eight horizontal railways in the east of the Hu Huanyong Line are much greater than in West China. Second, temporal and spatial distribution characteristics of hazards were analyzed using the data of geological hazards along the railway crawled through the network over the years. Apparently, geological hazards along the railway are on the rise year on year, with concentrated occurrence in June, July and August each year. Besides, the greatest impact on railway safety operation came from earthquakes (48%), followed by landslides (28%), debris flows (17%) and collapses (7%). Third, the susceptibility of geological hazards was modeled based on kernel density and information values. By overlaying with the geographical railway network, 4% of the lines in the network are exposed to highly susceptible (grade V) zones to geological hazards, and 26% are exposed to grade IV susceptible zones, which are mostly distributed in the southwest, northwest and northeast. Finally, the vulnerability of the railway section was analyzed based on the data of geological hazards along the railway and results of the susceptibility to geological hazards. The findings show that the most vulnerable railway lines include Sichuan–Guizhou Railway, Chengdu–Kunming Railway and Chengdu–Guizhou High-Speed Railway in Southwest China, Lanzhou–Urumqi Railway and Southern Xinjiang Railway in Northwest China, and Beijing–Harbin Railway and Harbin–Manzhouli Railway in Northeast China. Professional railway rescue materials should be arranged at

key stations at the above sections, including Harbin Station ($V_i = 0.0239$), Xining Station ($V_i = 0.0150$) and Qilongxing Station ($V_i = 0.0061$).

Although this paper analyzed the performance of the geographical railway network from the perspective of the prevention of sudden geological hazards and provides a scientific basis for the railway department to establish emergency plans, there are still some deficiencies. First, the cases of the geological hazards along the railway and the data concerning train stations used in this paper were all collected from publicly available information resources on the network, so omissions and mistakes are inevitable. Second, this paper did not obtain data on actual railway passenger flow, so it is difficult to analyze the network characteristics and vulnerability of the geographical railway network from the perspective of actual passenger flow, which should be further analyzed with more accuracy based on the collection of relevant data. Third, this paper mainly focused on the vulnerability of the railway lines. Social attributes (such as the economic losses caused) should also be considered in future research. Finally, only four typical geological hazards were selected for the research on the vulnerability of railway networks, so more hazards, such as typhoons and rainstorms, should be included in future research, and adopted scenario-specific simulations to analyze the vulnerability of major components of railway facilities should be conducted.

Author Contributions: Lingzhi Yin performed the experiments and wrote this paper; Jun Zhu and Wenshu Li provided important suggestions. Jinhong Wang reviewed and edited the manuscript. All authors have read and agreed to the published version of the manuscript.

Funding: This paper was supported by the National Natural Science Foundation of China under Grant No. 41801297; Science Foundation of Zhejiang Sci-Tech University (ZSTU) under Grant No. 20032312-Y.

Institutional Review Board Statement: Not applicable.

Informed Consent Statement: Not applicable.

Data Availability Statement: Not applicable.

Conflicts of Interest: The authors declare no conflict of interest.

References

- Ouyang, M.; Zhao, L.J.; Hong, L.; Pan, Z.Z. Comparisons of complex network-based models and real train flow model to analyze Chinese railway vulnerability. *Reliab. Eng. Syst. Saf.* **2014**, *123*, 38–46. [[CrossRef](#)]
- Hong, L.; Ouyang, M.; Peeta, S.; He, X.Z.; Yan, Y.Z. Vulnerability assessment and mitigation for the Chinese railway system under floods. *Reliab. Eng. Syst. Saf.* **2015**, *137*, 58–68. [[CrossRef](#)]
- Farooq, A.; Xie, M.; Stoilova, S.; Firoz Ahmad, F. Multicriteria evaluation of transport plan for high-speed rail: An application to Beijing-Xiongan. *Math. Probl. Eng.* **2019**, *2019*, 8319432. [[CrossRef](#)]
- Zhang, J.H.; Hu, F.N.; Wang, S.L.; Dai, Y.; Wang, Y.X. Structural vulnerability and intervention of high-speed railway networks. *Phys. A Stat. Mech. Appl.* **2016**, *462*, 743–751. [[CrossRef](#)]
- Wang, J.; Li, C.; Xia, C.Y. Improved centrality indicators to characterize the nodal spreading capability in complex networks. *Appl. Math. Comput.* **2018**, *334*, 388–400. [[CrossRef](#)]
- Farooq, A.; Xie, M.; Stoilova, S.; Ahmad, F.; Guo, M.; Williams, E.J.; Gahlot, V.K.; Yan, D.; Issa, A.M. Transportation planning through GIS and multicriteria analysis: Case study of Beijing and XiongAn. *J. Adv. Transp.* **2018**, *2018*, 2696037. [[CrossRef](#)]
- Ministry of Transport. Statistical Bulletin on the Development of the Transport Industry. 2020. Available online: https:////zjhy.mot.gov.cn/zzhxxgk/jigou/zghc/202105/t20210520_3595561.html (accessed on 25 September 2021).
- National Railway Administration. Notice on the Issuance of the “Medium- and Long-Term Railway Network Planning”. 2016. Available online: http://www.nra.gov.cn/xxgkml/xxgk/xxgkml/201908/t20190830_87801.shtml (accessed on 10 April 2019).
- Wu, W.J.; Liang, Y.T.; Di, W. Evaluating the Impact of China’s Rail Network Expansions on Local Accessibility: A Market Potential Approach. *Sustainability* **2016**, *8*, 512. [[CrossRef](#)]
- Ahmad, F.; Khan, S.A. Specification and verification of safety properties along a crossing region in a railway network control. *Appl. Math. Model.* **2013**, *37*, 5162–5170. [[CrossRef](#)]
- Yin, L.Z.; Wang, Y.F. Network Characteristics and Vulnerability Analysis of Chinese Railway Network under Earthquake Disasters. *ISPRS Int. J. Geo-Inf.* **2020**, *9*, 697. [[CrossRef](#)]
- Szymula, C.; Bešinović, N. Passenger-centered vulnerability assessment of railway networks. *Transp. Res. Part B Methodol.* **2020**, *136*, 30–61. [[CrossRef](#)]

13. Chen, X.Z.; Lu, Q.C.; Peng, Z.R.; Ash, J.E. Analysis of transportation network vulnerability under flooding disasters. *Transp. Res. Rec.* **2015**, *2532*, 37–44. [[CrossRef](#)]
14. Li, W.; Zhu, J.; Fu, L.; Zhu, Q.; Xie, Y.; Hu, Y. An augmented representation method of debris flow scenes to improve public perception. *Int. J. Geogr. Inf. Sci.* **2021**, *35*, 1521–1544. [[CrossRef](#)]
15. Eleutério, J.; Hattemer, C.; Rozan, A. A systemic method for evaluating the potential impacts of floods on network infrastructures. *Nat. Hazards Earth Syst. Sci.* **2013**, *13*, 983–998. [[CrossRef](#)]
16. Koseki, J.; Koda, M.; Matsuo, S.; Takasaki, H.; Fujiwara, T. Damage to railway earth structures and foundations caused by the 2011 off the Pacific Coast of Tohoku Earthquake. *Soils Found.* **2012**, *52*, 872–889. [[CrossRef](#)]
17. Kellermann, P.; Schöbel, A.; Kundela, G.; Thieken, A.H. Estimating flood damage to railway infrastructure—the case study of the March River flood in 2006 at the Austrian Northern Railway. *Nat. Hazards Earth Syst. Sci.* **2015**, *15*, 2485–2496. [[CrossRef](#)]
18. Liu, A.W.; Xia, S.; Xu, C. Damage and Emergency Recovery of the Transportation Systems after Wenchuan Earthquake. *Technol. Earthq. Disaster Prev.* **2008**, *3*, 243–250.
19. Zheng, Q.; Shen, S.L.; Zhou, A.N.; Cai, H. Investigation of Landslides that Occurred in August on the Chengdu–Kunming Railway, Sichuan, China. *Geosciences* **2019**, *9*, 497. [[CrossRef](#)]
20. Wang, W.W.; Li, Y.; Han, Z.; Li, M. Brief Analysis on the Establishment of Major Linear Engineering Geological Safety Monitoring and Early Warning System from the Derailment Accident of Train T179. *Urban Geol.* **2020**, *15*, 137–140.
21. Margat, J. *Vulnerability of Groundwater to Pollution*; BRGM: Orléans, France, 1968; pp. 6–7.
22. Timmerman, P. *Vulnerability, Resilience and the Collapse of Society: A Review of Models and Possible Climatic Application*; Institute for Environmental Studies: Toronto, ON, Canada, 1981; pp. 7–9.
23. Brooks, N.; Adger, W.N.; Kelly, P.M. The determinants of vulnerability and adaptive capacity at the national level and the implications for adaptation. *Glob. Environ. Chang.* **2005**, *15*, 151–163. [[CrossRef](#)]
24. Birkmann, J.; Cardona, O.D.; Carreño, M.L.; Barbat, A.H.; Pelling, M.; Schneiderbauer, S.; Kienberger, S.; Keiler, M.; Alexander, D.; Zeil, P.; et al. Framing vulnerability, risk and societal responses: The MOVE framework. *Nat. Hazards* **2013**, *67*, 193–211. [[CrossRef](#)]
25. Bell, M.G.H.; Kanturska, U.; Schmöcker, J.D.; Fonzone, A. Attacker–defender models and road network vulnerability. *Philos. Trans. R. Soc. A Math. Phys. Eng. Sci.* **2008**, *366*, 1893–1906. [[CrossRef](#)]
26. Berdica, K. An introduction to road vulnerability: What has been done, is done and should be done. *Transp. Policy* **2002**, *9*, 117–127. [[CrossRef](#)]
27. Hu, X.H.; Liu, Y. Traffic Vulnerability Analysis of the Road with Reserved Public Transportation Lane. *J. Transp. Eng. Inf.* **2006**, *4*, 128–133.
28. Erath, A.; Birdsall, J.; Axhausen, K.W.; Rade, H. Vulnerability assessment of the Swiss road network. In Proceedings of the 88th Transportation Research Board Annual Meeting, Washington, DC, USA, 11–15 January 2009; pp. 1–17.
29. Mattsson, L.G.; Jenelius, E. Vulnerability and resilience of transport systems—A discussion of recent research. *Transp. Res. Part A Policy Pract.* **2015**, *81*, 16–34. [[CrossRef](#)]
30. Albert, R.; Jeong, H.; Barabási, A.L. Error and attack tolerance of complex networks. *Nature* **2000**, *406*, 378–382. [[CrossRef](#)] [[PubMed](#)]
31. Cohen, R.; Erez, K.; Ben-Avraham, D.; Havlin, S. Breakdown of the internet under intentional attack. *Phys. Rev. Lett.* **2001**, *86*, 3682–3685. [[CrossRef](#)]
32. Berche, B.; von Ferber, C.J.; Holovatch, T.; Holovatch, Y. Resilience of public transport networks against attacks. *Eur. Phys. J. B* **2009**, *71*, 125–137. [[CrossRef](#)]
33. Wu, J.; Gao, Z.; Sun, H. Complexity and efficiency of Beijing transit network. *Int. J. Mod. Phys. B* **2006**, *20*, 2129–2136. [[CrossRef](#)]
34. Kermanshah, A.; Derrible, S. A geographical and multi-criteria vulnerability assessment of transportation networks against extreme earthquakes. *Reliab. Eng. Syst. Saf.* **2016**, *153*, 39–49. [[CrossRef](#)]
35. Candelieri, A.; Galuzzi, B.G.; Giordani, I.; Archetti, F. Vulnerability of public transportation networks against directed attacks and cascading failures. *Public Transp.* **2019**, *11*, 27–49. [[CrossRef](#)]
36. Pant, R.; Hall, J.W.; Blainey, S.P. Vulnerability assessment framework for interdependent critical infrastructures: Case-study for Great Britain’s rail network. *Eur. J. Transp. Infrastruct. Res.* **2016**, *16*, 174–194.
37. Meesit, R.; Andrews, J. Vulnerability assessment modelling for railway networks. In Proceedings of the 10th IMA International Conference on Modelling in Industrial Maintenance and Reliability, Manchester, UK, 13–15 June 2018. [[CrossRef](#)]
38. Khademi, N.; Balaei, B.; Shahri, M.; Mirzaei, M.; Sarrafi, B.; Zahabiun, M.; Mohaymany, A.S. Transportation network vulnerability analysis for the case of a catastrophic earthquake. *Int. J. Disaster Risk Reduct.* **2015**, *12*, 234–254. [[CrossRef](#)]
39. Binti Sa’adin, S.L.; Kaewunruen, S.; Jaroszweski, D. Heavy rainfall and flood vulnerability of Singapore–Malaysia high speed rail system. *Aust. J. Civ. Eng.* **2016**, *14*, 123–131. [[CrossRef](#)]
40. Zhao, J.; Liu, K.; Wang, M. Exposure analysis of Chinese railways to multihazards based on datasets from 2000 to 2016. *Geomat. Nat. Hazards Risk* **2020**, *11*, 272–287. [[CrossRef](#)]
41. Calzada-Infante, L.; Adenso-Díaz, B.; Carbajal, S.G. Analysis of the European international railway network and passenger transfers. *Chaos Solitons Fractals* **2020**, *141*, 110357. [[CrossRef](#)]
42. Cats, O.; Koppenol, G.J.; Warnier, M. Robustness assessment of link capacity reduction for complex networks: Application for public transport systems. *Reliab. Eng. Syst. Saf.* **2017**, *167*, 544–553. [[CrossRef](#)]

43. Cao, J.; Zhang, Z.; Du, J.; Zhang, L.; Song, Y.; Sun, G. Multi-geohazards susceptibility mapping based on machine learning—A case study in Jiuzhaigou, China. *Nat. Hazards* **2020**, *102*, 851–871. [[CrossRef](#)]
44. Wang, J.J.; Li, Y.S.; Liu, J.Y.; He, K.; Wang, P. Vulnerability analysis and passenger source prediction in urban rail transit networks. *PLoS ONE* **2013**, *8*, e80178. [[CrossRef](#)]
45. Mallick, J.; Singh, R.K.; AlAwadh, M.A.; Islam, S.; Khan, R.A.; Qureshi, M.N. GIS-based landslide susceptibility evaluation using fuzzy-AHP multi-criteria decision-making techniques in the Abha Watershed, Saudi Arabia. *Environ. Earth Sci.* **2018**, *77*, 276. [[CrossRef](#)]
46. Sun, C.S.; Cai, H.W. Developing and distributing characteristics of collapses and landslides during strong historic earthquake in China. *J. Nat. Disaster* **1997**, *6*, 25–30.
47. Matthews, M.V.; Ellsworth, W.L.; Reasenberg, P.A. A Brownian model for recurrent earthquakes. *Bull. Seismol. Soc. Am.* **2002**, *92*, 2233–2250. [[CrossRef](#)]
48. Vermeesch, P. On the visualization of detrital age distributions. *Chem. Geol.* **2012**, *312*, 190–194. [[CrossRef](#)]
49. Spencer, C.J.; Yakymchuk, C.; Ghaznavi, M. Visualising data distributions with kernel density estimation and reduced chi-squared statistic. *Geosci. Front.* **2017**, *8*, 1247–1252. [[CrossRef](#)]
50. Nandi, A.; Shakoor, A. A GIS-based landslide susceptibility evaluation using bivariate and multivariate statistical analyses. *Eng. Geol.* **2010**, *110*, 11–20. [[CrossRef](#)]
51. Bednarik, M.; Magulová, B.; Matys, M.; Marschalko, M. Landslide susceptibility assessment of the Kraľovany–Liptovský Mikuláš railway case study. *Phys. Chem. Earth Parts A/B/C* **2010**, *35*, 162–171. [[CrossRef](#)]
52. Galve, J.; Gutiérrez, F.; Remondo, J.; Bonachea, J.; Lucha, P.; Cendrero, A. Evaluating and comparing methods of sinkhole susceptibility mapping in the Ebro Valley evaporite karst (NE Spain). *Geomorphology* **2009**, *111*, 160–172. [[CrossRef](#)]
53. Zhou, G.; Yan, H.; Chen, K.; Zhang, R. Spatial analysis for susceptibility of second-time karst sinkholes: A case study of Jili Village in Guangxi, China. *Comput. Geosci.* **2016**, *89*, 144–160. [[CrossRef](#)]
54. Wu, Y.; Jiang, X.; Guan, Z.; Luo, W.; Wang, Y. AHP-based evaluation of the karst collapse susceptibility in Tailai Basin, Shandong Province, China. *Environ. Earth Sci.* **2018**, *77*, 436. [[CrossRef](#)]
55. Sharma, L.P.; Patel, N.; Ghose, M.K.; Debnath, P. Development and application of Shannon's entropy integrated information value model for landslide susceptibility assessment and zonation in Sikkim Himalayas in India. *Nat. Hazards* **2015**, *75*, 1555–1576. [[CrossRef](#)]
56. Zhao, H.L.; Yao, L.H.; Mei, G.; Liu, T.Y.; Ning, Y.S. A fuzzy comprehensive evaluation method based on AHP and entropy for a landslide susceptibility map. *Entropy* **2017**, *19*, 396. [[CrossRef](#)]
57. Singh, K.; Kumar, V. Hazard assessment of landslide disaster using information value method and analytical hierarchy process in highly tectonic Chamba region in bosom of Himalaya. *J. Mt. Sci.* **2018**, *15*, 808–824. [[CrossRef](#)]
58. Latora, V.; Marchiori, M. Efficient behavior of small-world networks. *Phys. Rev. Lett.* **2001**, *87*, 198701. [[CrossRef](#)] [[PubMed](#)]
59. Yao, S.B.; Jiang, D.B.; Fan, G.Z. Seasonality of Precipitation over China Chinese. *J. Atmos. Sci.* **2017**, *41*, 1191–1203.
60. Mas, J.-F.; Filho, B.S.; Pontius, R.G.; Gutiérrez, M.F.; Rodrigues, H. A suite of tools for ROC analysis of spatial models. *ISPRS Int. J. Geo-Inf.* **2013**, *2*, 869–887. [[CrossRef](#)]
61. Erkan, T.E.; Elsharida, W.M. Combining AHP and ROC with GIS for airport site selection: A case study in Libya. *ISPRS Int. J. Geo-Inf.* **2020**, *9*, 312. [[CrossRef](#)]